molecular pharmaceutics

articles

Immunological Effects and Membrane Interactions of Chitosan Nanoparticles

Aditya Pattani,[†,‡] Vandana B. Patravale,[*,‡] Lata Panicker,[§] and Pravin D. Potdar[*,†]

Department of Molecular Medicine and Biology, Jaslok Hospital and Research Centre, Mumbai-400026, India, Department of Pharmaceutical Science and Technology, Institute of Chemical Technology, Mumbai-400019, India, and Solid State Physics Division, Bhabha Atomic Research Centre, Mumbai-400049, India

Received June 16, 2008; Accepted January 19, 2009

Abstract: The objective of this study was to investigate the in vitro and in vivo effects of blank chitosan nanoparticles on various molecular markers such as nitric oxide (NO) production, IL-6 gene expression, and lymphocyte proliferation involved in the wound healing process. In addition, the membrane effects of chitosan nanoparticles were evaluated using phospholipid vesicles as a model membrane. Peripheral blood mononuclear cells (PBMC) were treated with blank chitosan nanoparticles, and the effect on NO production, IL-6 gene expression, and lymphocyte proliferation was evaluated. It was observed that IL-6 gene expression was not induced at any of the doses used; however, a statistically significant dose-dependent increase in NO production was observed at doses above 68.18 μg/mL equivalent to chitosan. Furthermore, chitosan nanoparticles showed a statistically significant and dose-dependent lymphocyte proliferation as compared to the control ($P < 0.05$). It was observed that blank chitosan nanoparticles resulted in strong membrane perturbation when evaluated by differential scanning calorimetry studies. The in vivo effects of the blank chitosan nanoparticles were evaluated using a wound healing model. Blank chitosan nanoparticles showed significantly higher NO production in vivo as compared to the control. Overall, the study clearly indicates the immunoactivating nature of chitosan nanoparticles and their strong membrane interactive potential.

Keywords: Chitosan nanoparticles; immunomodulation; interleukin-6; nitric oxide; lymphocyte; dipalmitoyl phosphatidylcholine membrane interactions

Introduction

With advances in nanoengineering and its applications, it is now clear that nanosystems are superior drug carriers that offer a variety of advantages including improved stability, improved antibody titers,[1] and efficient intracellular delivery,[2,3] for antimicrobials and vaccines.

Many of these advantages stem from the cell membrane interactions of nanoparticles and their immunomodulatory effects.[4−6] Chitosan nanoparticles have been used for a variety of immunological purposes including DNA vaccine carrier and adjuvant for effective immunization through

* Corresponding authors: Pravin D. Potdar, Head, Department of Molecular Medicine and Biology, Jaslok Hospital and Research Centre, 15 Dr. G. D. Deshmukh Road, Mumbai-400026, Maharashtra, India. Tel: 91-22-66573445. Fax: 91-22-23520508. E-mail: ppotdar@jaslokhopital.net. Vandana B. Patravale, Department of Pharmaceutical Science and Technology, Institute of Chemical Technology, Matunga, Mumbai-400019, Maharashtra, India. Tel: 91-22-24145616ext 2217. E-mail: vbpatravale@udct.org.

[†] Jaslok Hospital and Research Centre.

[‡] Institute of Chemical Technology.

[§] Bhabha Atomic Research Centre.

(1) Kreuter, J. Nanoparticle-based dmg delivery systems. *J. Controlled Release* **1991**, *16*, 169–176.

(2) Couvreur, P.; Fattal, E.; Andremont, A. Liposomes and Nanoparticles in the Treatment of Intracellular Bacterial Infections. *Pharm. Res.* **1991**, *8*, 1079–1086.

(3) Lecaroz, C.; Gamazo, C.; Blanco-Prieto, M. J. Nanocarriers with gentamicin to treat intracellular pathogens. *J. Nanosci. Nanotechnol.* **2006**, *6*, 3296–3302.

10.1021/mp900004b CCC: $40.75
Published on Web 03/06/2009

noninvasive nasal route.[7] It has also been demonstrated that coated chitosan nanoparticles may have potential for being used as a delivery system for oral vaccination with the recombinant hepatitis B surface antigen.[8] Further, porcine interleukin-2 (IL-2) gene encapsulated in chitosan nanoparticles is found to enhance immune response of mice to piglet paratyphoid vaccine.[9] Wound healing is an important immunological phenomenon. Chitosan based systems including polyelectrolyte complexes and polymeric networks have been extensively studied[10−12] and shown to affect many wound healing markers.[11] However, the effect of blank chitosan nanoparticles on various immunological markers involved in wound healing remains unknown. As a result, this study focuses on examining the in vitro effects of blank chitosan nanoparticles on wound immunological markers such as IL-6, nitric oxide (NO), and lymphocytes. Furthermore, the effect of blank chitosan nanoparticles on model membranes was studied. In order to substantiate the results obtained in vitro, we also examined the potential of blank chitosan nanoparticles to increase NO production in vivo in a wound healing model.

(4) Mottram, P. L.; Leong, D.; Crimeen-Irwin, B.; Gloster, S.; Xiang, S. D.; Meanger, J.; Ghildyal, R.; Vardaxis, N.; Plebanski, M. Type 1 and 2 immunity following vaccination is influenced by nanoparticle size: Formulation of a model vaccine for respiratory syncytial virus. *Mol. Pharmaceutics* **2007**, *4*, 73–84.
(5) Storni, T.; Kündig, T. M.; Senti, G.; Johansen, P. Immunity in response to particulate antigen-delivery systems. *Adv. Drug Delivery Rev.* **2005**, *57*, 333–355.
(6) Gomez, S.; Gamazo, C.; Roman, B. S.; Vauthier, C.; Ferrer, M.; Irache, J. M. Development of a novel vaccine delivery system based on Gantrez nanoparticles. *J. Nanosci. Nanotechnol.* **2006**, *6*, 3283–3289.
(7) Khatri, K.; Goyal, A. K.; Gupta, P. N.; Mishra, N.; Vyas, S. P. Plasmid DNA loaded chitosan nanoparticles for nasal mucosal immunization against hepatitis B. *Int. J. Pharm.* **2008**, *354*, 235–241.
(8) Borges, O.; Tavares, J.; de Sousa, A.; Borchard, G.; Junginger, H. E.; Cordeiro-da-Silva, A. Evaluation of the immune response following a short oral vaccination schedule with hepatitis B antigen encapsulated into alginate-coated chitosan nanoparticles. *Eur. J. Pharm. Sci.* **2007**, *32*, 278–290.
(9) Yang, Y.; Chen, J.; Li, H.; Wang, Y.; Xie, Z.; Wu, M.; Zhang, H.; Zhao, Z.; Chen, Q.; Fu, M.; Wu, K.; Chi, C.; Wang, H.; Gao, R. Porcine interleukin-2 gene encapsulated in chitosan nanoparticles enhances immune response of mice to piglet paratyphoid vaccine. *Comp. Immunol. Microbiol. Infect. Dis.* **2007**, *30*, 19–32.
(10) Hong, H.; Jin, S.; Park, J.; Ahn, W. S.; Kim, C. Accelerated wound healing by smad3 antisense oligonucleotides-impregnated chitosan/alginate polyelectrolyte complex. *Biomaterials* **2008**, *29*, 4831–4837.
(11) Ueno, H.; Mori, T.; Fujinaga, T. Topical formulations and wound healing applications of chitosan. *Adv. Drug Delivery Rev.* **2001**, *52*, 105–115.
(12) Kim, I. Y.; Yoo, M. K.; Seo, J. H.; Park, S. S.; Na, H. S.; Lee, H. C.; Kim, S. K.; Cho, C. S. Evaluation of semi-interpenetrating polymer networks composed of chitosan and poloxamer for wound dressing application. *Int. J. Pharm.* **2007**, *341*, 35–43.

Experimental Section

Preparation of Nanoparticle Dispersion. In-house purified chitosan (0.3 g; molecular weight 50,000 −60,000, 81.6% deacetylated; Healers Nutraceuticals, India) was dissolved in 49.7 g of 2% w/w lactic acid solution. To this, 3 g of Tween 80 (s.d. Fine Chemicals Ltd., Mumbai) and 1 g of Lutrol F-127 (BASF, GMbH, Germany) were added and stirred to dissolve. An aqueous solution of sodium carboxy methyl cellulose (sodium CMC), 40 g (0.17%; MW: 4000; Ideal Cures, India), was added to the chitosan solution very slowly under high speed stirring to yield chitosan nanoparticles. This dispersion was then neutralized to pH 5.2 using triethanolamine (s.d. Fine Chemicals Ltd., Mumbai). The volume was made up to 100 mL.

Size and Polydispersity of Nanoparticulate System. Photon correlation spectroscopy was used to determine the particle size and polydispersity of the nanoparticle dispersion. All measurements were performed using Beckman N4 Plus submicron particle size analyzer at a temperature of 20 °C ± 2 °C and at an angle of 90° to the incident beam on samples diluted 5-fold (v/v) in water. All data obtained were analyzed using the CONTIN program.

Isolation of Peripheral Blood Mononuclear Cells (PBMC). After obtaining an oral consent, blood was collected from healthy volunteers in heparin vacutainers (10 mL; 143 sodium heparin units, USP; B.D. Franklin Lakes, USA), and PBMC were isolated through Ficoll-Hypaque gradient centrifugation and adjusted to a concentration of 2×10^6 viable cells/mL in serum containing RPMI medium

Culture of PBMC and Stimulation with Nanoparticles. The cells were cultured in RPMI 1640 (HiMedia Laboratories, India) with 2 mM L-glutamine containing 10% of normal human serum (AB^{+ve}, heat-inactivated), 100 U/mL penicillin, 100 μg/mL streptomycin, 2.5 μg/mL amphotericin B, and 25 mM HEPES (HiMedia Laboratories, India). Cells were cultured in vitro in the presence of polymyxin B (60 μg/mL) for neutralizing any lipopolysaccharide contamination, which may give a false-positive immune response.

The nanoparticle dispersion was diluted in Hanks' balanced salt solution and 100 μL of it was added to the culture to obtain the final concentration of chitosan (Table 1).

Table 1. Final Concentration of Chitosan in the Cell Culture Medium (μg/mL)

group (code)	final concn of chitosan in μg/mL
1 (control)	0
2 (40 μL T)	54.5
3 (50 μL T)	68.18
4 (60 μL T)	81.8

Cultures were incubated at 37 ± 1 °C in 5% CO_2 for 24 h. The cells were then used for viability analysis and viable nonadherent cell (lymphocyte) count, and for RNA extraction for IL-6 gene expression analysis. The supernatants were immediately frozen at −70 °C and used for nitric oxide analysis. The control used for comparison in all the in vitro

and in vivo experiments was a solution that contained sodium CMC, Lutrol F-127, Tween 80 and lactic acid as mentioned above.

Lymphocyte Cell Count. The nonadherent (suspended) cells were separated and counted using the trypan blue dye exclusion method, using a hemocytometer.

Extraction of RNA and Conversion to cDNA. RNA was isolated from a combined population of adherent and nonadherent cells using Trizol reagent (Invitrogen Life Technologies, USA) according to the manufacturer's instructions. cDNA was prepared from 1 μg of RNA using a RevertAid cDNA synthesis kit (Fermentas Life Sciences, USA) according to the manufacturer's instructions.

PCR for IL6 and Actin Gene Expression. The cDNA was analyzed using PCR. The primer sequences for IL-6 were used as described by Poels et al.,[13] and PCR was performed using DFS-Taq DNA Polymerase (Bioron GmbH) according to the manufacturer's instructions. Primer sequences were as follows: for IL-6, sense, 5′-GTCTCCTCATTGAATCCAGATTGG-3′; antisense, 5′ AGCTCAGCTATGAACTCCTTCTC-3′; for β-actin, sense, 5′ GACTACCTCATGAAGATC-3′; antisense, 5′ GATCCACATCTGCTGGAA-3′ were obtained from Sigma Genosys, India. The PCR reaction mixture also consisted of 0.01% bovine serum albumin. PCR was initiated in a thermal cycler (DNA Engine Dyad Peltier Thermal Cycler, M J Research, USA) programmed at 94 °C for 1 min and 40 cycles of denaturation for 1 min at 94 °C, annealing for 1 min at 58 °C, and extension for 1 min at 72 °C. This was followed by a final extension of 7 min. The expected sizes of the PCR products for IL-6 and β-actin were 338 and 512 bps, respectively. The PCR products were visualized on a 2% agarose gel.

Estimation of Nitric Oxide in Cell Culture Supernatants. Nitric oxide was measured using the Griess reaction based on a procedure reported by Govindarajan et al.[14] Culture supernatant (300 μL) was mixed with 300 μL of Griess reagent (1% sulfanilamide in 5% phosphoric acid and 0.1% *N*-(1-naphthyl)ethylenediamine dihydrochloride). The mixture was incubated at room temperature for 10 min. Absorbance values of test samples were measured at 570 nm using a spectrophotometer (UV 1601 spectrometer, Shimadzu, Japan), and the amount of nitric oxide liberated was calculated as nitric oxide equivalent based on a sodium nitroprusside standard curve.

Nanoparticles−DPPC Membrane Interactions. Dipalmitoyl phospatidyl choline (DPPC) vesicles were used as artificial membranes because of their biomimetic properties.[15] Multilamellar vesicles (MLV) of DPPC (25 mM) were formed by lipid film hydration method. The lipid film was hydrated with pH 5.2 phosphate buffer. A thorough dispersion of DPPC in the buffer was achieved by heating in a water bath maintained 10 °C above the chain-melting transition temperature and vortexed at room temperature. This procedure was repeated at least 10 times. To this DPPC dispersion, blank chitosan nanoparticles were added in a 1:1 weight ratio and the effect of nanoparticles was analyzed using a differential scanning calorimeter (DSC 822^e, Mettler Toledo) with a heating rate of 5 °C/min as a function of time (t). For DSC measurement, 10−15 mg of MLV with or without nanoparticles was hermetically sealed in aluminum pans. The Mettler Toledo DSC 822^e differential scanning calorimeter was also used for thermal measurements of the membrane samples, with an empty aluminum pan as a reference. Temperature and enthalpy calibration of the instrument was performed using cyclohexane and indium at a heating rate of 10 °C/min. The chain-melting (CM), transition temperature (T_m), and transition enthalpy (ΔH_m) of the DPPC membrane were obtained using the heating endothermic curve. The full width at half-maximum (Δ_m) used to compare the cooperativity of the CM transitions was obtained from 5 °C/min scans. Following the preparation of MLV, experiments were immediately conducted and were repeated till maximum interaction occurred (∼106 min).

Wound Excision Model. The protocol used was approved by the institutional ethical committee. The SD rats weighing between 250−300 g was used. The rats were anesthetized prior to the induction of wounds with 50 mg/kg of Thiopentone sodium ip. An excision wound was created, and the animals were divided into three groups, each containing three animals. Animals in group 1 were treated with normal saline (1 mL) and considered as the control. Group 2 was treated with a solution (1 mL) containing sodium CMC, Lutrol, and lactic acid, which served as a blank. Group 3 was treated with chitosan nanoparticles (1 mL). The wounds were covered with gauze and dressed. After 24 h, each of the wounds was sampled and the samples were divided into two sections—one toward the periphery of the wound and one away from the periphery. Samples for histopathology were stored in 10% formalin solution, and those for estimation of NO were frozen at −20 °C.

Histopathology. Wound tissue was routinely processed and embedded in paraffin. Paraffin sections (5 μm) were cut on glass slides and stained with hematoxylin and eosin (HE). The sections were observed under a microscope using 10× and 40× objectives. Immunostimulation, as a function of leukocyte infiltration, was evaluated by a veterinary pathologist blinded to the study.

In Vivo Estimation of NO. In vivo NO production was measured using the Griess reaction based on a procedure reported by Govindarajan et al.[14] Homogenized wound tissue from two areas of the wound per animal (animals = 3, sample size = 6) were homogenized in chilled normal saline (NS), and the concentration of tissue was adjusted to 30 mg

(13) Legrand-Poels, S.; Schoonbroodt, S.; Piette, J. Regulation of interleukin-6 gene expression by pro-inflammatory cytokines in a colon cancer cell line. *Biochem. J.* **2000**, *349*, 765–773.

(14) Govindarajan, R.; Vijaykumar, M.; Rawat, A. K. S.; Mehrotra, S. Free Radical Scavenging Potential of Picrorhiza kurrooa Royle ex Benth. *Indian J. Exp. Biol.* **2003**, *41*, 875–879.

(15) Ventura, C. A.; Tommasini, S.; Crupi, E.; Giannone, I.; Cardile, V.; Musumeci, T.; Puglisi, G. Chitosan microspheres for intrapulmonary administration of moxifloxacin: Interaction with biomembrane models and in vitro permeation studies. *Eur. J. Pharm. Biopharm.* **2008**, *68*, 235–244.

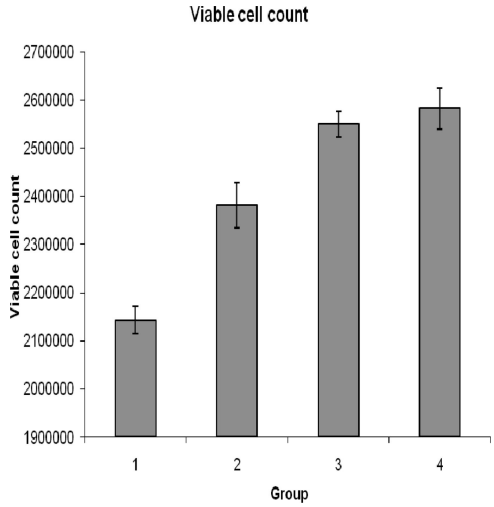

Figure 1. The average viable lymphocyte after treatment for 24 h. Group 1 (control), group 2 (treatment with chitosan nanoparticles equivalent to chitosan (54.5 μg/mL), group 3 (treatment with chitosan nanoparticles equivalent to chitosan (68.18 μg/mL), and group 4 (treatment with chitosan nanoparticles equivalent to chitosan (81.8 μg/mL). The lymphocyte proliferation at all doses was significant ($P < 0.001$).

of tissue per mL. Of this, 1 mL was taken and centrifuged, and the supernatant, 300 μL, was mixed with 300 μL of Griess reagent. The mixture was incubated at room temperature for 30 min. Absorbance values of test samples at 570 nm were measured using a spectrophotometer (UV 1601 spectrometer, Shimadzu, Japan) and a suitable blank. The amount of nitric oxide liberated was calculated as NO equivalents based on a sodium nitroprusside standard curve.

Results

Size and Polydispersity of Nanoparticulate System. The particle size of the developed nanoparticulate system was 373.1 nm with a polydispersity index of 0.696.

PBMC Culture and Stimulation with Nanoparticles. The PBMC could be cultured without contamination. After incubation at various concentrations, the average viability was more than or equal to 90%.

Lymphocyte Cell Count. The cell count of nonadherent PBMC, which reflected the lymphocyte population, was determined. The experiment was repeated in triplicate with samples obtained from three volunteers. Figure 1 describes the results of the total viable cell count, and error bars indicate the standard deviations. The results were further analyzed using one-way ANOVA followed by Tukey's test to compare the individual columns.

The nanoparticles induced significant lymphocyte proliferation ($P < 0.05$) at all doses; however, proliferation flattens off at high doses. Negative controls (blank containing same concentrations of sodium CMC, Lutrol F-127, Tween 80, and lactic acid) at all the doses were also used for the study. The blank showed no statistically significant ($P > 0.05$) lymphocyte proliferation at any dose.

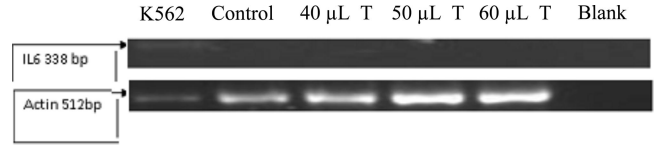

Figure 2. PCR products for IL6 and actin gene expression.

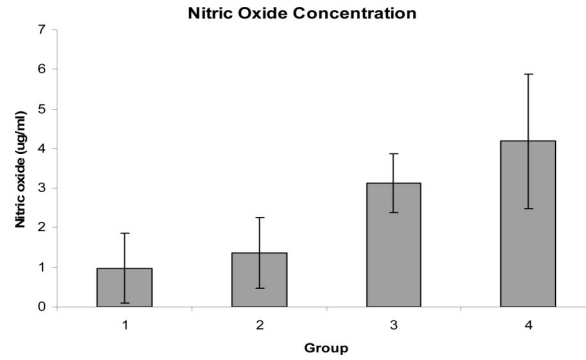

Figure 3. Nitric oxide amounts in PBMC supernatants after 24 h. Group 1 (control), group 2 (treatment with chitosan nanoparticles equivalent to chitosan 54.5 μg/mL, group 3 (treatment with chitosan nanoparticles equivalent to chitosan 68.18 μg/mL), and group 4 (treatment with chitosan nanoparticles equivalent to chitosan 81.8 μg/mL. The nitric oxide production in groups 3 and 4 was significant ($P < 0.05$) as compared to the control.

PCR for IL-6 and Actin Gene Expression. Figure 2 shows the gel lanes of the PCR products for β-actin (a housekeeping gene) and IL-6.

The presence of an actin band in all samples indicates the integrity of the synthesized cDNA. Absence of bands in the blank indicated that it was free of contamination. The positive control for IL-6, cDNA from k562 cell line, was successful, indicating that the PCR conditions were satisfactory. Absence of bands in PBMC cells treated with nanoparticles indicated no detectable induction of IL-6 gene expression. Absence of any band in the blank IL-6 PCR indicated absence of contamination. Further, no IL-6 gene expression was seen in the blank at any dose.

Nitric Oxide Estimation in Culture Supernatant. The NO equivalents detected in the cell culture supernatant for each group are shown in Figure 3 with the error bars indicating the standard deviation. The results were further analyzed using one-way ANOVA followed by Tukey's test to compare the individual columns.

Blank chitosan nanoparticles showed significantly higher ($P < 0.05$) NO production from PBMC cells, as compared to control and the solution that contained a mixture of sodium CMC, Lutrol F-127, Tween 80, and lactic acid all at the same concentration as that present in the nanoparticles. This clearly indicates that the effect on the NO production was attributed to the chitosan nanoparticles.

Nanoparticles−DPPC Membrane Interactions. The DSC heating profiles obtained at a scan rate of 5 °C/min of DPPC dispersion (MLV) containing nanoparticles for dif-

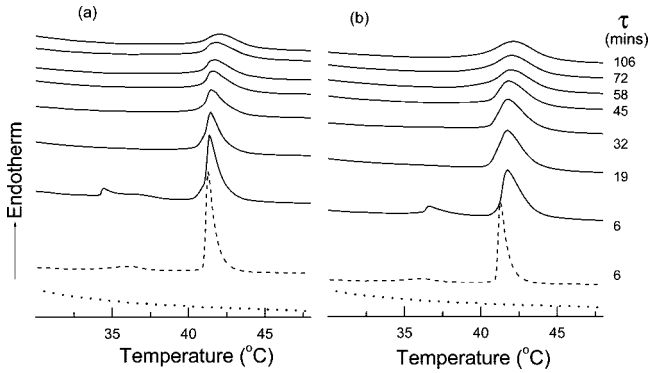

Figure 4. The DSC heating profiles at 5 °C/min of (a) nanoparticles (dotted curves), DPPC−buffer pH 5.2 (dash curve), and DPPC−nanoparticles−buffer pH 5.2 (solid curve). (b) Blank (dotted curves), DPPC−buffer pH 5.2 (dash curve), and DPPC−blank−buffer pH 5.2 (solid curve) at different equilibration time τ.

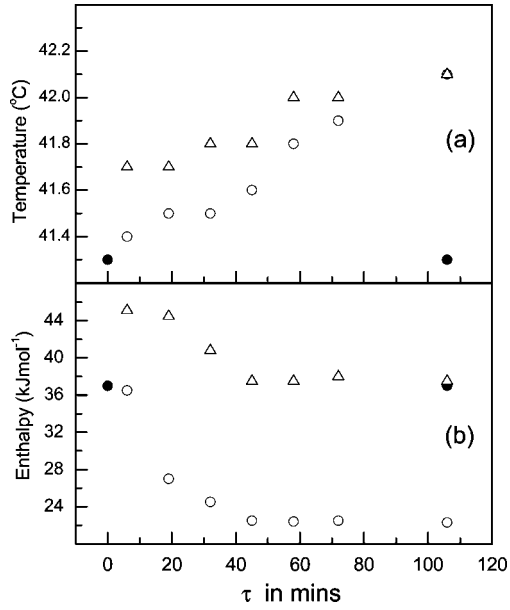

Figure 5. (a) Transition temperature and (b) transition enthalpy (kJ·mol^{-1}) of DPPC−buffer pH 5.2 (filled circles), DPPC−blank−buffer pH 5.2 (open triangles), and DPPC− nanoparticles−buffer pH 5.2 (open circles) systems as a function of equilibration time τ.

ferent times are given in Figure 4. The blank DPPC MLV scan results are also provided for comparison. The corresponding time dependence of the thermotropic parameters; the transition temperatures, T_{PT} and T_m; and the transition enthalpies, ΔH_{PT} and ΔH_m, are given in Figures 5a and 5b, respectively.

The gel phase of DPPC dispersion displays two endothermic transitions—the pretransition (PT) and the CM transition—in the DSC heating profile (Figure 4).

PT (T_{PT}) was observed at 36.1 °C, and enthalpy, ΔH_{PT}, associated with this transition was 4.0 kJ·mol^{-1}. Chain-melting transition was observed at temperature, $T_m = 41.3$ °C, and the associated enthalpy, ΔH_m, was 37.0 kJ·mol^{-1}. The value of these thermal parameters is in good agreement with those reported in literature.[16,17] The nanoparticles did not show any thermal transition from 20 to 50 °C.

Figure 4 shows that the incorporation of nanoparticles in DPPC dispersion perturbs the thermotropic properties of DPPC vesicles and this perturbation is time (τ)-dependent. Pretransition was observed during the first scan ($\tau = \sim 6$ min), but disappeared during the second scan taken at $\tau = \sim 19$ min. This suggests a possible interaction between nanoparticles and the polar head groups of DPPC, leading to changes in the gel $L_{\beta'}$ phase (indicated by inhibition of ripple phase in the DSC scan). From the acyl chain-melting transition, it was observed that with increasing time the transition broadened and the transition temperature, T_m, shifted to higher value (Figures 5a and 5b).

Figure 5 shows that the transition enthalpy, ΔH_m, of DPPC−nanoparticle dispersion decreases with time. This perturbation in the thermal values gets saturated with time. Hence, for time $\tau > 52$ min, no further change in the thermal values is observed.

The model membranes undergo a transition (the main transition) corresponding to the chain melting transition or the gel to liquid crystalline phase transition at temperature T_m. For temperature, $T < T_m$ the acyl chains are in an extended trans conformation and the chains form a regular 2-D ordered lattice in the lamellae. The membrane is rigid in this ordered (gel) phase (L_β or $L_{\beta'}$) hence not allowing diffusion of even small molecules through it. At T_m, the acyl chains melt leading to a disordered packing of the chains in the lamellae, and hence this transition can be considered as the melting of a 2-D crystal to a 2-D liquid. The disordered phase known as the liquid crystalline (L_α) phase allows diffusion of small molecules through the membrane.

In the presence of nanoparticles, formation of the ripple phase is inhibited as indicated by the disappearance of the PT.

The ripple phase formation is known to be very sensitive to the presence of foreign molecules.[18,19] The physical nature of the L_β phase has been further explained elaborately in several studies.[16−19]

The ripple phase inhibition suggests that nanoparticles are localized near the polar headgroup of the lipid and interacts via hydrogen bonding or/and by electrostatic attraction. From the chain melting transition, it is seen that the CM transition broadens and its transition temperature (T_m) increases and enthalpy (ΔH_m) decreases with time. The increase in T_m value suggests that the nanoparticles increased the headgroup

(16) Huang, C.; Li, S. Calorimetric and molecular mechanics studies of the thermotropic phase behavior of membrane phospholipids. *Biochim. Biophys. Acta* **1999**, *1422*, 273–307.
(17) Koynova, R.; Caffrey, M. Phases and phase transitions of the phosphatidylcholines. *Biochim. Biophy. Acta* **1998**, *1376*, 91–145.
(18) Bertoluzza, A.; Bonora, S.; Fini, G.; Francioso, O.; Morelli, M. A. Interaction of bipyridilium herbicides with model membranes. *Chem. Phys. Lipids* **1995**, *75*, 137–143.
(19) Biltonen, R. L.; Lichtenberg, D. The use of differential scanning calorimetry as a tool to characterize liposome preparations. *Chem. Phys. Lipids* **1993**, *64*, 129–142.

Table 2. Level of Leukocyte Infiltration

treatment	level of leukocyte infiltration
NS	mild
CMC blank	mild
chitosan nanoparticles	moderate

rigidity. The broadening of the CM transition is indicative of a reduction in the cooperativity among the lipid acyl chains. These results suggest that the nanoparticles could get intercalated between the lipid polar head groups by forming hydrogen bonds and/or by electrostatic interaction and also penetrate into the cooperative region. Steady decrease in enthalpy values indicates increase in disorder of chains making the system amenable to penetration into the membrane.

From the DSC data, it is seen that the negative control (a mixture of sodium CMC, Lutrol F-127, Tween 80 and lactic acid) also interacts with DPPC vesicles (Figure 4b). However, the interaction is more with nanoparticle as indicated by reduction in the transition enthalpy with time (Figure 5b). The reduced enthalpy value of the chain melting transition of DPPC suggests that nanoparticles penetrate into the acyl chain region of the lipid. While in DPPC treated with blank system, molecules are located in the polar headgroup region.

Histopathology. The overall impression shows a higher leukocyte infiltration into the wound area, indicating greater immunostimulation by the nanoparticles compared to blank and normal saline control. The histopathologic evaluations are indicated in Table 2 (see also Figure 6).

Nitric Oxide Production. The wounded tissue, when treated with the nanoparticles, shows much higher levels of nitric oxide (statistically significant, $P < 0.05$) compared to the blank, corroborating that the data that was obtained in vitro. The levels are shown in Figure 7.

Discussion and Conclusion

PBMC cultures were treated with the nanoparticles at concentrations 0−81.8 μg/mL for 24 h. Various effects of the nanoparticles on these cells at the cellular and molecular levels were studied, and further in vivo studies were carried out to corroborate the results.

The first marker used was IL-6. In our study, chitosan nanoparticles did not show any changes in the IL-6 gene expression in PBMC cells at a noncytotoxic concentration. A survey of literature shows that solid lipid nanoparticles when used at low concentrations did not affect the secretion of IL-6 in murine peritoneal macrophages,[20] while titanium dioxide nanoparticles caused elevated levels of IL-6 when exposed to a cultured human bronchial cell line.[21] A detailed study on the effect of hydroxyapatite nanoparticles on human monocytes has been reported.[22,23] The results indicate that the levels of IL-6 secretion by the monocytes depend upon

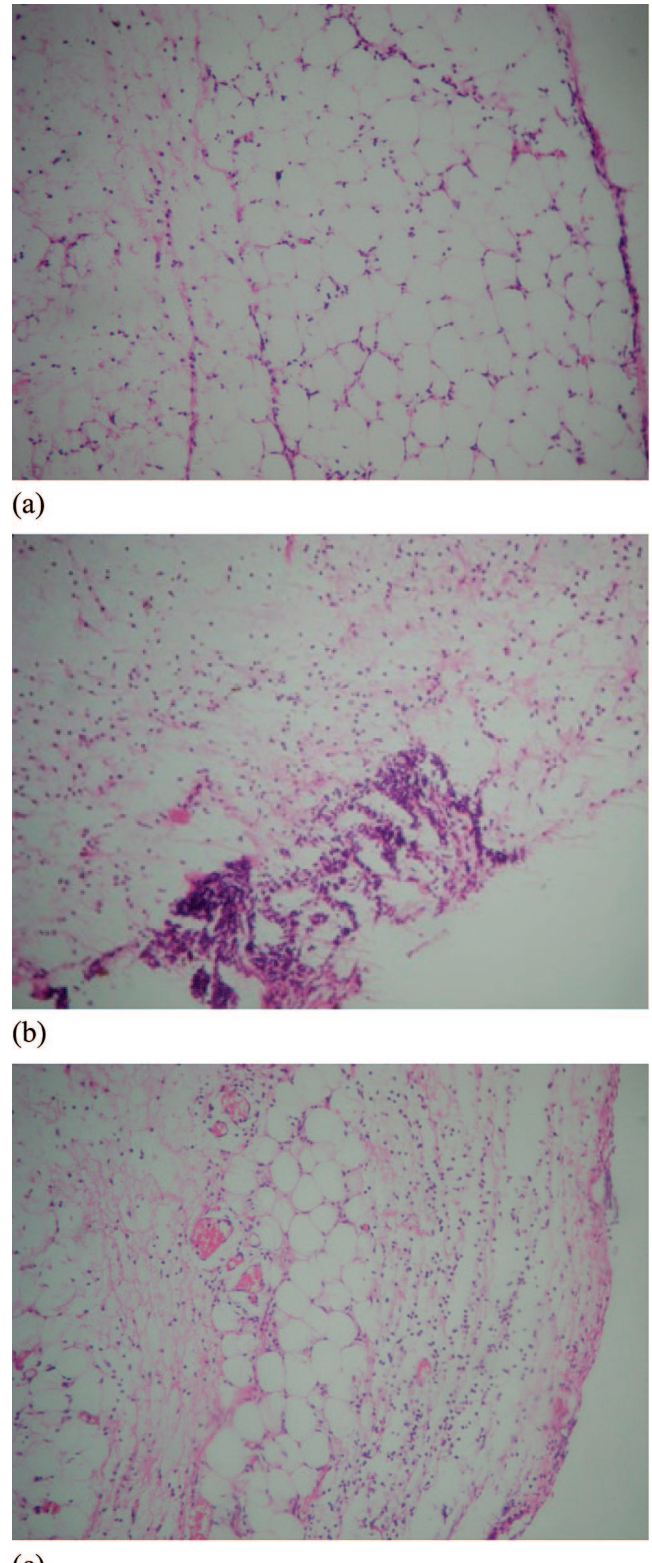

Figure 6. Histopathological evaluation after treatment with (a) normal saline, (b) blank solution containing sodium CMC, Lutrol, and lactic acid, and (c) chitosan nanoparticles. Note: Panel b shows a necrotic patch in the lower half.

physical characteristics of the particles. Chitosan nanoparticles complexed with DNA when treated exposed to THP

(20) Scholer, N.; Zimmermann, E.; Katzfey, U.; Hahn, H.; Muller, R. H.; Liesenfeld, O. Effect of solid lipid nanoparticles (SLN) on cytokine production and the viability of murine peritoneal macrophages. *J. Microencapsulation* **2000**, *17*, 639–650.

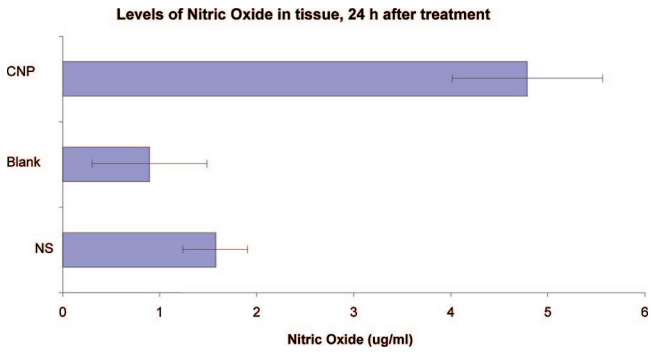

Figure 7. Nitric oxide levels after treatment with (a) normal saline (NS), (b) blank solution containing sodium CMC, Lutrol, and lactic acid, and (c) chitosan nanoparticles (CNP). Only chitosan nanoparticles showed a statistically significant increase in nitric oxide production ($P < 0.001$).

1 human cell line, showed no change in IL-6 secretion.[24] However, a precise comparison of the results obtained is not possible as different cell types have been used, but it is clear that material and physical attributes of the particle affect the secretion of IL-6. Furthermore, we studied the production of nitric oxide by the PBMC when treated with the nanoparticles. At higher concentrations, the nanoparticles induced the liberation of nitric oxide from PBMC cells. This is in contrast to a study which suggested that chitosan microspheres did not have any effect on nitric oxide production in vitro.[25] This difference could possibly result from inefficient internalization of chitosan microparticles; whereas the nanoparticles used in this study had a high potential for internalization as shown by the interaction with model membranes.

The nanoparticles caused lymphocyte proliferation in a dose-dependent manner, but not in a dose-proportional manner. Further, as the concentration of nanoparticles increased, there was a concomitant increase in the nitric oxide production; however, the lymphocyte proliferation alleviates possibly because of the antiproliferative nature of nitric oxide toward lymphocytes.[26]

Several studies have used chitosan nanoparticles as very efficient vehicles for immunoactives.[7,9,27] Although the "carrier" property of chitosan nanoparticles has been studied widely, the immunostimulation produced by the nanoparticles has not been exploited. Also, a molecular characterization of such an immunostimulation is not evident. The current study shows that the chitosan nanoparticles have significant immunostimulatory effects as observed in case of various immune-markers such as NO and lymphocyte proliferation.

The observation that the nanoparticles induce lymphocyte proliferation bolsters the use of chitosan nanoparticles as vaccine adjuvants. Moreover, the fact that these nanoparticles induce liberation of nitric oxide indicates their potential use for antimalarial therapy and treatment of tuberculosis, since nitric oxide inhibits the growth of *Plasmodium falciparum* and has also been shown to have antiplasmodial and antimycobacterial activity.[28−30] Besides general immunostimulation, these specific markers are important markers for immune activity at the wound site. The wound is essentially an immunologically active site. Using the wound as a model immunologically active area, a cutaneous wound was treated with the nanoparticles. There were a significant increase in nitric oxide levels at the wound site and a significant increase in the infiltration of leukocytes, which shows clearly the immunostimulation produced by these nanoparticles.

Nitric oxide also promotes wound healing through angiogenesis, migration of epithelial cells, keratinocyte prolifera-

(21) Park, E.; Yi, J.; Chung, K.; Ryu, D.; Choi, J.; Park, K. Oxidative stress and apoptosis induced by titanium dioxide nanoparticles in cultured BEAS-2B cells. *Toxicol. Lett.* **2008**, *180*, 222–229.

(22) Grandjean-Laquerriere, A.; Laquerriere, P.; Guenounou, M.; Laurent-Maquin, D.; Phillips, T. M. Importance of the surface area ratio on cytokines production by human monocytes in vitro induced by various hydroxyapatite particles. *Biomaterials* **2005**, *26*, 2361–2369.

(23) Laquerriere, P.; Grandjean-Laquerriere, A.; Jallot, E.; Balossier, G.; Frayssinet, P.; Guenounou, M. Importance of hydroxyapatite particles characteristics on cytokines production by human monocytes in vitro. *Biomaterials* **2003**, *24*, 2739–2747.

(24) Chellat, F.; Grandjean-Laquerriere, A.; Naour, R. L.; Fernandes, J.; Yahia, L.; Guenounou, M.; Laurent-Maquin, D. Metalloproteinase and cytokine production by THP-1 macrophages following exposure to chitosan-DNA nanoparticles. *Biomaterials* **2005**, *26*, 961–970.

(25) Luzardo-Alvarez, A.; Blarer, N.; Peter, K.; Romero, J. F.; Reymond, C.; Corradin, G.; Gander, B. Biodegradable microspheres alone do not stimulate murine macrophages in vitro, but prolong antigen presentation by macrophages in vitro and stimulate a solid immune response in mice. *J. Controlled Release* **2005**, *109*, 62–76.

(26) Fecho, K.; Maslonek, K.; Coussons-Read, M.; Dykstra, L.; Lysle, D. Macrophage-derived nitric oxide is involved in the depressed concanavalin A responsiveness of splenic lymphocytes from rats administered morphine in vivo. *J. Immunol.* **1994**, *152*, 5845–5852.

(27) Bivas-Benita, M.; van Meijgaarden, K. E.; Franken, K. L. M. C.; Junginger, H. E.; Borchard, G.; Ottenhoff, T. H. M.; Geluk, A. Pulmonary delivery of chitosan-DNA nanoparticles enhances the immunogenicity of a DNA vaccine encoding HLA-A*0201-restricted T-cell epitopes of Mycobacterium tuberculosis. *Vaccine* **2004**, *22*, 1609–1615.

(28) Gyan, B.; Troyeblomberg, M.; Perlmann, P.; Bjorkman, A. Human Monocytes Cultured with and without Interferon-Gamma Inhibit Plasmodium-Falciparum Parasite Growth In-Vitro Via Secretion of Reactive Nitrogen Intermediates. *Parasite Immunol.* **1994**, *16*, 371–375.

(29) Mellouk, S.; Hoffman, S. L.; Liu, Z. Z.; Delavega, P.; Billiar, T. R.; Nussler, A. K. Nitric Oxide-Mediated Antiplasmodial Activity in Human and Murine Hepatocytes Induced by Gamma-Interferon and the Parasite itself - Enhancement by Exogenous Tetrahydrobiopterin. *Infect. Immun.* **1994**, *62*, 4043–4046.

(30) Chan, E. D.; Chan, J.; Schluger, N. W. What is the role of nitric oxide in murine and human host defense against tuberculosis? Current knowledge. *Am. J. Res. Cell Mol. Biol.* **2001**, *25*, 606–612.

tion, and collagen secretion by fibroblasts.[31] Lymphocytes are known to actively participate in the wound healing process.[32] The strong interaction of the nanoparticles with the model membrane indicates a possible reason for improved antimicrobial activity (unpublished data). Further, the enthalpy study indicates the possibility that the nanoparticles could deliver drugs intracellularly to treat intracellular infections including *Pseudomona*s infections known to occur in open wounds, thus bolstering the use of chitosan nanoparticles as immunostimulating wound healing agents.

In conclusion, drug-free chitosan nanoparticles show strong immunoactivating properties and can activate various factors that promote wound healing, besides the indication that they may help to improve intracellular drug delivery and potentiate actions of antibiotics.

Acknowledgment. The authors wish to thank Mrs. Naina Rane, Mr. Milind Chanekar, Mr. Devang Shah and Mr. Abhijit Date for their guidance. Also thanked are University grants commission for funding the research, as well as Healers Nutraceuticals, Ideal cures Ltd and HiMedia Laboratories Pvt. Ltd for the gift samples of various chemicals and excipients.

MP900004B

(31) Yamasaki, K.; Edington, H. D. J.; McClosky, C.; Tzeng, E.; Lizonova, A.; Kovesdi, I.; Steed, D. L.; Billiar, T. R. Reversal of impaired wound repair in iNOS-deficient mice by topical adenoviral-mediated iNOS gene transfer. *J. Clin. Invest.* **1998**, *101*, 967–971.

(32) Cole-King, A.; Harding, K. G. Psychological factors and delayed healing in chronic wounds. *Psychosom. Med.* **2001**, *63*, 216–220.